DOIGNON François (Orcid ID: 0000-0002-9007-2408)

Phosphoinositides containing stearic acid are required for interaction between Rho GTPases and the exocyst to control the late steps of polarised exocytosis

P. Laquel[1], E. Testet[1], K. Tuphile[1], C. Cullin[2] https://orcid.org/0000-0003-4110-4677, L. Fouillen[1,3] https://orcid.org/0000-0002-1204-9296, J.J. Bessoule[1] https://orcid.org/0000-0002-5717-5210 and F. Doignon[1*]https://orcid.org/0000-0002-9007-2408

[1] *Univ. Bordeaux, CNRS, Laboratoire de Biogenèse Membranaire, UMR 5200, F-33140 Villenave d'Ornon, France*

[2] *Univ. Bordeaux, CNRS, Laboratoire de Chimie Biologie des Membranes & des Nano-objets, UMR 5248, F-33607 Pessac, France*

[3] *Metabolome Facility of Bordeaux, Functional Genomics Centre, F-33883 Villenave d'Ornon, France*

* Corresponding author: francois.doignon@u-bordeaux.fr

Summary

Cell polarity is achieved by regulators such as small G proteins, exocyst members and phosphoinositides, with the latter playing a key role when bound to the exocyst proteins Sec3p and Exo70p, and Rho GTPases. This ensures asymmetric growth via the routing of proteins and lipids to the cell surface using actin cables. Previously, using a yeast mutant for a lysophosphatidylinositol acyl transferase encoded by the *PSI1* gene, we demonstrated the role of stearic acid in the acyl chain of phosphoinositides in cytoskeletal organisation and secretion. Here, we use a genetic approach to characterise the effect on late steps of the secretory pathway. The constitutive overexpression of *PSI1* in mutants affecting kinases involved in the phosphoinositide pathway demonstrated the role of molecular species containing stearic acid in bypassing a lack of phosphatidylinositol-4- phosp hate PI(4)P at the plasma membrane, which is essential for the function of the Cdc42p module. Decreasing the levels of stearic acid-containing phosphoinositides modifies the environment of the actors involved in the control of late steps in the secretory pathway. This leads to decreased interactions between Exo70p and Sec3p, with

This article has been accepted for publication and undergone full peer review but has not been through the copyediting, typesetting, pagination and proofreading process which may lead to differences between this version and the Version of Record. Please cite this article as doi: 10.1111/tra.12829

Cdc42p, Rho1p and Rho3p, due to disruption of the GTP/GDP ratio of at least Rho1p and Rho3p GTPases, thereby preventing activation of the exocyst.

1 Introduction

Maintenance of cell polarity is an essential biological process shared by all eukaryotic cells, ensuring asymmetric growth by routing proteins and lipids to specific sites on the cell surface. The transport of secretory vesicles and many intracellular organelles is dependent on the presence of polarised actin cables that radiate from the bud cortex and the neck, extending into the mother cell[1]. Polarised secretion is spatially and temporally regulated by many different actors, such as small G proteins[2], exocyst members[3] and phosphoinositides[4,5]. The quantitative modification of pools of different phosphoinositides affects trafficking processes[6-8], due to the control of late steps of the secretory pathway by some Rho GTPases that modulate the docking of vesicles in concert with the exocyst complex[2,9,10]. Phosphoinositides play a key role in these steps by being simultaneously bound to exocyst subunits Sec3p and Exo70p and to some members of Rho GTPase modules[4,11,12]. In a previous study, we characterised a yeast strain carrying a mutation in lysophosphatidylinositol acyltransferase, leading to qualitative modification of the phosphoinositide molecular species. We demonstrated the role of the acyl chain of phosphoinositides, specifically stearic acid, in the organisation of the actin cytoskeleton and the secretory pathway[13].

In the present paper, we first characterised the step(s) of the secretory pathway affected by a lack of phosphoinositides containing stearic acid using genetic approaches. The constitutive overexpression of the *PSI1* gene in strains carrying mutations in genes encoding kinases involved in the phosphoinositide pathway demonstrated the role of molecular species containing stearic acid in bypassing a lack of PI(4)P, an essential phosphoinositide for the polarisation of the Cdc42p module[14]. We further show that changes in the composition of the acyl chains of phosphoinositides modify the environment of actors involved in the control of late steps of the secretory pathway. In addition, using a Bimolecular Fluorescence Complementation (BiFC) assay approach, we demonstrate that these changes lead to a decrease in interactions between exocyst components Exo70p and Sec3p, and Rho GTPases (Cdc42p, Rho1p and Rho3p). This marked decrease in the interactions observed between Rho proteins (Rho1p, Rho3p and Cdc42p)

and the plasma membrane-bound exocyst subunits (Exo70p and Sec3p) is induced by a disruption in the GTP/GDP ratio of Rho proteins, preventing activation of the exocyst.

2 Results

2.1 Phosphoinositides containing stearic acid are required for the control of late steps of the secretory pathway

Secretion assays have demonstrated that protein trafficking is disturbed in mutants for the lysophosphatidyl acyltransferase *psi1*Δ[13], but do not demonstrate which stage of the trafficking is disturbed. To address this point, we first investigated genetic interactions between the *PSI1* and *SEC* genes involved in the secretory pathway. We created double-mutant strains deficient in *PSI1* and harbouring a panel of heat-sensitive *sec* mutations affecting the activity of the translocon (*sec62-1*)[15,16], signal peptide processing (*sec11-7*)[17], the guanine exchange factor (GEF) of the small GTPase Sar1p involved in anterograde trafficking (*sec12-1*)[18,19], the GEF of Arf members, the GTPases regulating anterograde and retrograde traffic from the TGN (*sec7-1*)[20,21]. Furthermore, genetic links with an R-SNARE localised in the ER (endoplasmic reticulum) and the Golgi apparatus and involved in anterograde and retrograde transport by controlling membrane fusion (*sec22*Δ)[22,23] were carried out. We also analysed a putative functional link between *PSI1* and the function of the Golgi apparatus via the phosphatidylinositol/phosphatidylcholine transfer protein (*sec14-1*)[24,25] and the late steps of trafficking controlled by the Rho protein (*cdc42-6*)[26] or a member of the exocyst (*sec6-4*)[21,27]. Finally, a cryosensitive mutant (*rho3-V51*)[28] affecting another member of the Rho GTPase family, also regulating the late stages of exocytosis, was studied. Likewise, mutation of other genes was used to generate double-mutants with the *PSI1* deletion. These genes include those involved in ER-to-Golgi apparatus[29] and Golgi apparatus-to-ER protein recycling (*erd1*Δ)[30], and an endocytosis internalisation step linked to actin patch function (*end3*Δ)[31,32].

Comparisons of the growth of double-mutants (*sec, psi1*Δ) and single-mutants (*sec*) were performed using serial dilutions and spotting on complete media at permissive, intermediate and non-permissive temperatures (Figures 1A, B, C). Remarkably, at 30°C, the *psi1*Δ mutation behaved as a suppressor of *sec7-1*. Sec7p is a GEF for Arf1p and Arf2p, which are known to facilitate COPI (Coat Protein I) and clathrin-coating dynamics at the Golgi apparatus and

function in many different steps of intracellular trafficking, such as retrograde transport from the Golgi apparatus to the ER and anterograde transport to the lysosome and vacuole (Figure 1B)[33]. Growth of the *sec22*Δ *psi1*Δ double-mutant was impaired at 37°C relative to the single mutant *sec22*Δ (Figure 1C) but did not show a decrease in cell viability observed using the methylene blue staining method (data not shown)[34]. The strains *sec62-1 psi1*Δ (at permissive and intermediate temperatures, Figure 1A, 1B) and *rho3-V51 psi1*Δ (at a permissive temperature, Figure 1A) displayed a slight growth defect compared to the single *sec* mutants. A synergetic effect was observed between the *rho3-V51* allele and *psi1*Δ only at 25°C, based on a cell lethality of 20 ± 2.4% for the double-mutant and 12 ± 1.9% for the *rho3* single-mutant. These data suggested that Psi1p may interact functionally *in vivo* with some proteins involved in exocytosis, mainly during the docking of secretory vesicles to membranes and particularly during the final steps of trafficking. Moreover, the growth of *cdc42-6* was strongly affected at 30°C when *PSI1* deletion was present alongside this conditional mutation (Figure 1B). Cell lethality at 30°C was estimated at 32 ± 5% for the double-mutant, compared to 8 ± 1% for the single mutant *cdc42-6*. This synthetic lethality observed between *cdc42-6* and *psi1*Δ revealed that *PSI1* and *CDC42* are genetically linked and involved in the same pathway(s) regulating secretion.

Growth assays performed on a strain with a mutation in another allele of *CDC42* (*cdc42-1*) only showed a weak effect on secretion but demonstrated impairment of the dynamics of the actin cytoskeleton[26,35,36]. We also analysed *cdc42-1* to determine the specificity of the *cdc42-6* allele in showing synthetic lethality with *psi1*Δ. The comparison of the single mutant and double-mutant *cdc42-1 psi1*Δ did not demonstrate any synergistic effect on growth in the double-mutant (Figure S1). These results show that *PSI1* only genetically interacted with the *CDC42* allele that is involved in secretion, but not with the allele involved in actin dynamics.

2.2 The growth defect observed in *cdc42-6* can be rescued by constitutive overexpression of *PSI1*

To further investigate the links between *PSI1* and genes involved in intracellular trafficking, the *PSI1* ORF (Open Reading Frame) was constitutively overexpressed using the pCM189 plasmid[37] in the different secretory mutants described in section 2.1. No significant growth difference was

observed for these secretory mutants, either with the pCM189 plasmid containing the *PSI1* gene or with the empty vector, except for the *cdc42-6* strain, where the weak growth at 30°C was rescued by constitutive overexpression of the *PSI1* gene at the intermediate temperature (30°C) (Figure 2). This result combined with the synthetic lethality between *cdc42-6* and *psi1*Δ suggests a balancing effect between the action of Cdc42p and phosphoinositides with stearic acyl chains at the plasma membrane. Interestingly, previous work showed that the *cdc42-6* mutant could also be rescued by overexpression of the kinase encoded by *MSS4*, which is involved in PI(4,5)P_2 biosynthesis[7].

2.3 Constitutive overexpression of *PSI1* can suppress the reduced growth of the *stt4-4ts* kinase mutant by increasing the level of PIP 36:0

Various studies demonstrate the role of phosphoinositides in intracellular trafficking[8,11,38-42]; therefore, we aimed to analyse the links between the genes involved in phosphoinositide synthesis and the *PSI1* gene. The plasmid pCM189 (either the empty vector or carrying the *PSI1* gene for constitutive overexpression) was used to transform the conditional mutant strains that affect phosphoinositide synthesis: AAY104 *(pik1-83ts)*[8], AAY102 *(stt4-4ts)*[38] and AAY202 *(mss4-102ts)*[43]. *PSI1* overexpression seems to suppress the growth defect at 30°C of strains when compared with the empty vector, the effect is remarkably strong with *stt4-4ts* mutant (deficient in plasma membrane PI4-kinase) (Figure 3). The *mss4-102ts* and the *pik1-83ts* mutants like the wild-type strain show a much smaller effect, suggesting that the *PSI1* overexpression potentially improves the growth of these strains. This could suggest a more general effect of *PSI1* overexpression on cell fitness.

To understand the suppressor effect of *PSI1* in the *stt4-4ts* mutant, new strains (either overexpressing *PSI1* or not) expressing a PI(4,5)P_2 biosensor, GFP-2xPH$^{PLC\delta 144}$, were constructed in *stt4-4ts* and wild-type backgrounds. In the *stt4-4ts* mutant at a permissive temperature (25°C), the distribution of the GFP-2xPH$^{PLC\delta 1}$ biosensor was shown using confocal microscopy to be located predominantly at the growth site in a similar range (47 ± 4%) to that observed in the wild-type strain (62 ± 9%) (Figures 4A and B). By contrast, after shifting to a non-permissive temperature (30 °C) for one hour, the GFP-2xPH$^{PLC\delta 1}$ biosensor revealed drastic modifications in topology for PI(4,5)P_2. Notably, the cells had a PI(4,5)P_2 topology defect at the

growth site, with these molecular species located at the growing site for only 13 ± 5% of the polarised cells. *PSI1* overexpression induced $PI(4,5)P_2$ re-localisation to the growth area for 46 ± 5% of the *stt4-4ts* cells at 30°C, a value similar to that observed under permissive conditions (Figures 4A and B). The ratios of the amount of $PI(4,5)P_2$-specific reporter detected on the plasma membrane at the growing site (bud tip and bud neck) compared to the rest of the mother cell's body was 1.03 ± 0.10 at 30°C for the *stt4-4^{ts}* mutant with the empty plasmid pCM189. This reflects a uniform localisation of the probe at the plasma membrane between the bud and the mother cell. This ratio was 1.42 ± 0.18 with the pCM189-*PSI1* plasmid, indicating the enrichment of the $PI(4,5)P_2$ probe at growth areas (Figure 4C).

To understand the role of overexpression of the *PSI1* gene in rescuing the *stt4-4ts* mutation, the proportions of different phosphoinositide species were analysed using LC-MS/MS (liquid chromatography-tandem mass spectrometry) (Figures 5A, B and C). A dramatic 35% decrease in PIP 36:0 levels was observed specifically for the *stt4-4ts* strain transformed with the empty plasmid and grown at a non-permissive temperature (30°C). The levels were restored when the *PSI1* gene was constitutively overexpressed at this temperature (Figure 5B). No decrease in the levels of PIP 36:0 was observed at 30°C for the reference strain SEY6210 when transformed with the empty vector (Figure 5E). When the *PSI1* gene was overexpressed in the SEY6210 strain, an increase of 81% at 25°C and 93% at 30°C was observed for PIP2 36:1 (Figure 5F). This increase was correlated with the increase in PIP 36:1 (90% at 25°C and 63% at 30°C). More generally, in the SEY6210 parental strain, levels of molecular species of PI, PIP and PIP2 containing stearic acid 34:1; 36:0 and 36:1 were increased following overexpression of *PSI1*, whereas in the mutant strain *stt4-4ts* this increase was restricted to PIP 36:0 and PIP2 36:1.

To determine if the suppressive effect of the *PSI1* gene overexpression is due only to a qualitative effect of the PIP pool on the cell, we performed steady-state lipid labelling using [1-^{14}C]acetate. This was carried out in *stt4-4ts* strains with the *PSI1* gene either overexpressed or expressed at normal levels, at permissive and non-permissive temperatures. After the purification of lipids by HPTLC (High-Performance Thin Layer Chromatography) followed by quantification of their radioactivity, we did not detect any increase in PIP levels when *PSI1* was overexpressed (Figure S2). This result shows that a qualitative effect of the PIP pool is responsible for the suppressive effect of the *PSI1* gene.

2.4 Phosphoinositides containing stearic acid are required to maintain certain polarity landmarks associated with a specific membrane environment, but do not cause changes in membrane fluidity

To analyse the association of tagged cellular landmarks involved in cell polarity with features of the membrane environment, crude cell extracts were subjected to a 0–40% discontinuous density gradient of OptiPrep™ by ultracentrifugation, in both a *psi1*Δ/*psi1*Δ genetic background and in the reference strain. The tagged landmarks were revealed by Western blot using an anti-HA antibody (Figure 6). For both exocyst complex subunits that interact with $PI(4,5)P_2$ through a polybasic region (Exo70p and Sec3p)[39,45,46] and for the landmarks Cdc42p and Rho1p (belonging to the Rho family), a shift in the sedimentation velocity was observed between the mutant strain and the control. This suggests that the membrane environment of these secretory landmarks was modified when stearic acid was absent from the phosphoinositides (Figure 6). In contrast, no disturbance in the sedimentation profile was observed for Rho3p.

PI is a major phospholipid in *S. cerevisiae*[47] and it is possible that modification of the acyl chain could alter membrane fluidity. In order to investigate any link between the membrane environment and fluidity, generalised polarisation (GP) indices were calculated using the fluorescent dye laurdan, a sensitive membrane dynamics probe used to measure the degree of membrane order[48-51]. The GP indices of the wild-type strain and the *psi1*Δ mutant deficient for the synthesis of phosphoiniositides with stearic acid were similar, indicating a comparable degree of membrane order (Figure S3). Hence, the secretory pathway in the *psi1*Δ mutant was not impacted via modification of membrane fluidity.

2.5 Interactions between Rho GTPases and members of the exocyst are dependent on the presence of phosphoinositides containing stearic acid

The exocyst complex is composed of eight subunits (Sec3p, Sec5p, Sec6p, Sec8p, Sec10p, Sec15p, Exo70p and Exo84p) and is involved in the fusion of secretory vesicles with the plasma membrane. Furthermore, the exocyst determines the region of the plasma membrane where exocytosis takes place[3]. Cdc42p interacts with Exo70p[52] and Sec3p[45], Rho1p with Sec3p[53] and Rho3p with Exo70p[54]. The exocyst subunits (except Sec3p) are associated with the vesicles

before they migrate to the bud tip[9]. The localisation of Sec3p to the tip of small buds at the plasma membrane is independent of the actin cytoskeleton involved in the secretory pathway[55]. Two populations of Exo70p exist, the first in transit with vesicles and the second distributed in a manner similar to Sec3p[9].

To investigate any disruption of the interactions between the Rho GTPases and exocyst subunits Exo70p and/or Sec3p, we established a BiFC assay. Cdc42p, Rho1p and Rho3p were tagged at their N-terminal ends with a C-terminal fragment of the fluorochrome Venus (VC) using a single-step PCR strategy with the pFA6a-His3MX6-P_{CET1}-VC plasmid, the transcription being controlled by the *CET1* promoter[56]. Conversely, Exo70p and Sec3p were tagged at their C-terminal with the N-terminal part of Venus (VN) using the pFA6a-VN-His3MX6 plasmid, allowing regulation of their expression by their native promoters[56]. We quantitatively analysed the BiFC signal for all constructions co-expressing VC-Rho and exocyst-VN using a flow cytometry-based approach. As shown in Figure 7A, a marked decrease in relative fluorescence intensity compared to the reference strain was observed in each of the four combinations for the *psi1*Δ mutant (from 78% of decrease for VC-Cdc42/Exo70-VN up to 89% for VC-Rho1/Sec3-VN). This indicates a substantial disruption of the interactions between the Rho GTPases and the exocyst proteins.

In order to determine whether the decrease in fluorescence was due to a limited number of protein-protein interaction events per cell or a limited number of cells in the population exhibiting these interaction events, we conducted confocal microscopy analysis of the cells. For each of the four recombinant strains co-expressing VC-Rho and exocyst-VN, a dramatic decrease (47–93%) in the proportion of cells showing a specific BiFC signal at the growing area was observed in the *psi1*Δ mutant (Figure 7B). The strongest decrease (93%) was observed for the Rho1p-Sec3p interaction. Thus, in the absence of phosphoinositides with C18:0, fewer cells in the population exhibit an interaction between the Rho proteins and the exocyst subunits known to bind $PI(4,5)P_2$ (Sec3p or Exo70p)[45,52-54]. In order to prove that Rho GTPase/exocyst interactions were dependent on the *PSI1* gene, rescue via the overexpression of *PSI1* was implemented in strains deleted for *PSI1*. *psi1*Δ/*psi1*Δ strains expressing the *PSI1* gene carried by pCM189 plasmid, showed a strong increase in the proportion of cells with a specific fluorescent signal at the bud-tip or the bud-neck for all four combinations compared to cells carrying the

empty plasmid (Figure S4). This clearly shows that Rho GTPase/Exocyst interactions are dependent on the presence of stearic acid containing phosphoinositides.

As expected, the BiFC fluorescent signal was only observed at the growth area and scored both in the reference strain and the *psi1*Δ genetic background for each of the four tested combinations (Figure S5A). For the combination VC-Rho3/Exo70-VN, a low fluorescent signal was observed due to the weak pool of Rho3p detected in the bud tip[52,57]. No specific fluorescent signal was observed by confocal microscopy at the bud tip or at the bud neck in the strains expressing either *VC-CDC42*, *VC-RHO1*, *VC-RHO3* paired with VN alone or *EXO70-VN*, *SEC3-VN* with VC alone demonstrating that the fluorochrome fragments VC and VN cannot reconstitute a functional fluorochrome by themselves, but require the specific interaction between Rho proteins and exocyst partners (Figure S5B).

In order to prove that differences observed in fluorescence intensity were due to a decrease in the interaction between Rho and the exocyst and not to an effect of the *psi1* mutation on the expression of chimeric genes with reporters, RT-qPCR experiments were performed. The results demonstrate that the depletion of phosphoinositides containing stearic acid did not impact the activity of the *CET1*, *EXO70*, and *SEC3* promoters (Figure S6). Therefore, the decrease of cells in the population with a BiFC signal was induced by a decrease of the Rho/Exocyst interactions.

2.6 The localisation of Exo70p and Sec3p is not disturbed in the *psi1*Δ mutant

Based on the observation that the interaction between the Rho proteins and the exocyst was reduced in the *psi1*Δ genetic background, we hypothesised that this phenotype could be explained by a mislocalisation of the Rho and exocyst proteins. Therefore, we investigated whether the lack of phosphoinositides containing stearic acid could affect the localisation of either Exo70p or Sec3p by confocal microscopy of strains expressing GFP-tagged proteins (Figure S7A). In three independent experiments, we did not observe any abnormal localisation of either exocyst subunit: Exo70p and Sec3p were distributed in similar proportions at the bud tip, at 77% and 75%, respectively, for the wild-type cells and at 75% and 72%, respectively, for the *psi1*Δ mutant cells (Figure S7B). Hence, despite the BiFC assay demonstrating that the

interactions between Cdc42p and Exo70p and between Cdc42p and Sec3p decreased in *psi1*Δ background, no alteration in exocyst subunit localisation was highlighted.

Cdc42p cellular distribution was also analysed using a GFP-Cdc42 plasmid. We quantified the localisation of GFP-Cdc42p in wild-type and *psi1* mutant cells and measured the GFP fluorescence localised in the early emerging bud cells. A slight difference was highlighted in this case, with 71 ± 3% of *psi1*Δ cells showing localisation of GFP-Cdc42p to the bud tip compared to 84 ± 4% in the WT strain (Figure S7B). Thus, similarly to the *cdc42-6* mutant[26], a slight decrease in localization at the bud tip for Cdc42p was revealed, in contrast to the exocyst proteins Exo70 and Sec3, for which no modification was revealed. This suggest that the lack of interaction of the exocyst proteins with Cdc42p was not induced by a wrong localization of the exocyst proteins, but can be due in part to a slight alteration of the localization of a key factor of polarization, namely Cdc42p.

2.7 The activation states of Rho1p, Rho3p are affected by the lack of stearic acid in phosphoinositides, and perhaps to a lesser extent for Cdc42p.

Previous work has shown that interactions between the Exo70p or Sec3p subunits with Rho proteins are restricted to their GTP-bound active state[53,54,58]. Our work showed that in a genetic context characterised by the lack of stearic acid in the phosphoinositides, a marked decrease in the interaction between exocyst subunits and key factors in intracellular trafficking occurred. We hypothesised that PI(4,5)P_2 containing stearic acid (C18:0) is essential for the control of late steps in trafficking by interacting with key polarisation factors such as Cdc24p, (a RhoGEF of Cdc42p), Rga1/2p and Bem2/3p (several RhoGAPs for Cdc42p[59,60]); Rom2p (the RhoGEF of Rho1p, another member of the Rho family interacting with Sec3p[53,61]) and/or Rgd1p (the RhoGAP for Rho3p interacting with the exocyst[28,62,63]).

Therefore, aiming to detect alterations of the GTP/GDP ratio of Rho GTPases, we performed an *in vivo* test based on pull-down analysis assays to determine the proportion of the GTP-bound, activated form of the Rho GTPases in the different strains. We used either the RBD (Rho Binding Domain) domain from rhotekin fused to a GST-tag for affinity precipitation of Rho1p[64] and Rho3p[65], or the CRIB (Cdc42/Rac Interacting Domain) domain from Ste20p fused to a GST-tag in the case of Cdc42p[66]. 3xHA-Rho-GTP-bound proteins were pulled down from cell extracts

prepared from cells grown in SC (Synthetic Complete) lacking uracil and methionine (to induce the production of either 3xHA-Rho1p, 3xHA-Rho3p or 3xHA-Cdc42p). Specific antibodies raised against Pgk1p were used to estimate the total amount of protein loaded onto the gels. RBD- or CRIB-tagged GSTs were used to determine the amount of beads loaded[64] (Figure 8A). The amount of each protein was determined using band intensity quantification. For each experiment, the total amount of Rho proteins was determined and normalised to the total amount of protein loaded. Similarly, the amount of GTP-Rho was determined and normalised to the total amount of GST-RBD or GST-CRIB. The ratios of these normalised values were calculated. For each Rho protein, results from the mutant strain were normalised to the wild-type strain.

The ratio of Rho pull-down to total Rho in extracts from the strains expressing the blocked GTP-bound GTPases was 6.70 ± 2.54, 3.24± 2.28 and 1.08 ± 0.33 for Rho1p, Rho3p, and Cdc42p, respectively (Figure 8B), demonstrating the efficiency of the pull-down assay for Rho1p and Rho3p, but less evidently for Cdc42p for which we did not observe a significant accumulation of the blocked GTP-bound GTPase, despite the many analyses carried out and probably related to the use in our hands of the Ste20-CRIB domain. The ratios of the activated Rho proteins to the total Rho proteins in the *psi1*Δ mutant were 0.72 ± 0.05, 0.62 ± 0.10 and 0.50 ± 0.52 for Rho1p, Rho3p and Cdc42p, respectively, when normalised to the WT strain. This result unambiguously demonstrates that the *PSI1* gene deletion, causing a lack of phosphoinositides with stearic acid, induced a decrease in the GTP-forms of at least two Rho proteins namely Rho1 and Rho3. But it also appears that, for Cdc42p, differences between WT and *psi1*Δ strains were not statistically significant. In other words in our hands the repeatability of the pull down assay for Cdc42p was unsatisfactory. Nevertheless results shown in Figure 8B could suggest that a decrease also in the amount of Cdc42-GTP could occur in *psi1*Δ strain.

3 Discussion

Our results show that the presence of PI C18:0 catalysed by the *PSI1* gene product is necessary for the correct functioning of the secretory pathway at the vesicle docking step. The strongest genetic interaction was between *PSI1* and a specific allele of *CDC42,* mainly affecting trafficking (*cdc42-6*), but not with another allele causing disturbance in actin polarisation (*cdc42-1*)[26,36]. This shows that the *PSI1* deletion preferentially affects Cdc42p functions

involving secretory pathway partners, rather than protein partners involved in actin cytoskeleton dynamics. Previous results have demonstrated the accumulation of cargo with Bgl2p in the internal un-secreted pool for *cdc42-6,* as well for *sec6-4,* and *rho3-V51*[26,28]. A modified version of the Bgl2p-HA secretion assay suitable for the detection of disturbances in the early stages of the cell cycle[67] also revealed a secretion defect in the *psi1*Δ strain[13]. Thus, we analysed genetic interactions between *PSI1* and genes involved in vesicle docking during exocytosis. The genetic interactions we have demonstrated between *PSI1* and *CDC42* or *RHO3,* encoding two key proteins involved in the late steps of polarised exocytosis, are consistent with previous results based on the Bgl2p secretion assay, showing an accumulation of Bgl2p-HA in an endocellular fraction at the early bud stage in the *psi1*Δ mutant. Furthermore, a mild synergic effect was highlighted between *PSI1* and a thermosensitive allele of *SEC62,* a gene encoding a member of the translocon complex involved in the early steps of trafficking. This is in agreement with previous results highlighting a link between the early and late steps of trafficking, more precisely between members of the exocyst (Sec4p, Sec8p and Sec15p) and Seb1p, a subunit of the translocon[68,69].

In a yeast strain carrying a *PSI1* deletion, the decrease in fatty acyl chains with stearic acid in phosphoinositides generates strong perturbations of cell polarity[13]. The cell polarity is also highly disturbed in the *Caenorhabditis elegans acl-10* mutant (an orthologous gene of *PSI1*), since the percentage of cells with abnormal seam orientation during cell division is strongly increased. In the triple mutant for the three orthologous genes *acl-8, acl-9* and *acl-10,* which encode lysophosphatidylinositol acyltransferases, an abnormal seam orientation was also observed. In agreement with our results, a suppressor effect of this phenotype was revealed in a quadruple mutant disrupted for *acl-8, acl-9, acl-10* and the ArfGEF *mon-2*, belonging to the Sec7 family and involved in retrograde trafficking[70]. In addition, physical and functional links between *SEC7* and *PIK1* (involved in PI(4)P synthesis to coordinate Arf activation) were previously highlighted[71]. Our results demonstrated a similar genetic link between *SEC7* (coding also for an ArfGEF) and *PSI1*, which is involved in phosphoinositide synthesis.

In *S. cerevisiae*, two pools of PI(4)P are synthesised in the Golgi apparatus and plasma membrane by two essential type III PI 4-kinases, Pik1p and Stt4p, respectively[8,72]. The pool of PI(4)P specifically synthesised by Stt4p is essential for recruiting both the Cdc42p GTPase module itself[14] and Cla4p, an activator downstream of Cdc42p involved in septin hourglass

formation[73,74]. *PSI1* overexpression induced the overproduction of PIP (36:0), and in the *stt4-4ts* mutant at 30°C, the amount of this molecular species grows up to 15% to the level observed at permissive temperatures. In comparison, PIP (36:0) production increases by only 9% in the *stt4-4ts* mutant (without *PSI1* overexpression) when grown at 30°C. It was also shown that the bulk of the PI(4,5)P_2 produced at the plasma membrane by the PI(4)P-kinase Mss4p is dependent on Stt4p activity[75]. By recruiting two subunits of the exocyst, Sec3p and Exo70p, in cooperation with Cdc42p[7,39,45], Rho1p[53] and Rho3p[54], PI(4,5)P_2 is required for secretory vesicle docking and fusion with the plasma membrane[40]. In our work, using a PI(4,5)P_2 biosensor, we observed that, in the *stt4* mutant, a pool of PI(4,5)P_2 was present at the plasma membrane, but excluded from the growth area at the non-permissive temperature. This mislocalisation of PI(4,5)P_2 in the *stt4-4ts* mutant has been previously described at a non-permissive temperature in yeast during shmoo formation[76]. Unlike mammalian cells[77], we did not find an intracellular compartment containing PI(4,5)P_2 in *stt4-4ts* yeast at a non-permissive temperature.

The Cdc42p GTPase module, including the guanine exchange factor Cdc24p, the scaffold Bem1p and the kinase Cla4p, bind to the PI(4)P, PI(4,5)P_2 and PS (phosphatidylserine) pools in the plasma membrane. Together, these components make it possible for Bem1p and Cdc24p to localise to the membrane and for Cdc42p to be activated by GTP[14,78]. The constitutive overexpression of *PSI1* should rescue the lethality of *stt4-4ts* by maintaining a pool of PI(4)P with stearic acid PIP (36:0) at the plasma membrane (Figure 5B). This pool may be required for the function of this module, a lack of PIPs containing stearic acid being detrimental to the late steps of secretion due to either a slight decrease in the activity of Cdc42p or/and its reduced localization to the growth area. Moreover, the high proportion of PIP (36:0) may induce the greater localisation of PI(4,5)P_2 to the growth zone (Figure 4), suppressing the effect of the *stt4-4ts* mutation to some degree.

Looking at the sedimentation profiles of Exo70p and Sec3p using OptiPrep™ density gradients, we observed intriguing differences between the *psi1*Δ/*psi1*Δ strain and the control (Figure 6). Sedimentation of cell extracts using the gradient exhibited a shift in the *psi1*Δ/*psi1*Δ strain compared to the control for both Rho1p and Cdc42p, but not for Rho3p (Figure 6). Interestingly, in contrast with Rho3p, the C-terminal domains of Rho1p[79] and Cdc42p[14,80] contain a polybasic region enriched in positively charged amino acids (lysine) that interacts with phosphoinositides and PS.

Sec3p and a pool of Exo70p are located at polarised growth sites independent of the secretory pathway, which uses actin cables[9]. These subunits bind to the inner leaflet of the plasma membrane at PIP2 clusters[12]. Exo70p binds to the GTP-activated forms of Cdc42p and Rho3p[54], while Sec3p binds to the activated forms of Cdc42p[45,58] and Rho1p[53]. Exo70p and Sec3p act in concert to mediate the anchorage of secretory vesicles to the plasma membrane via other exocyst subunits[39,53]. In the *mss4* strain (mutated for PI(4,5)P_2 kinase) Sec3p and Exo70p are mislocalised, emphasising the role of PI(4,5)P_2 in polarised growth[7,39]. In contrast with the *mss4* temperature-sensitive mutant, our work shows that the deficiency of phosphoinositides with stearic acid does not disturb the localisation of either Exo70p or Sec3p; however, we did observe a slight modification of the subcellular localisation of Cdc42p at the bud tip (13% less compared to the wild-type strain). In the *rho3-V51* strain, the interaction of Rho3p with Exo70p was decreased[54] and a marked decrease in the interaction between Cdc42p with Exo70p was shown in the *cdc42-6* strain *in vitro*[54]. Interactions of Rho3p with Exo70p and Cdc42p with Sec3p are not essential for growth at the permissive temperature[39,45], but the thermosensitive mutations *cdc42-6* or *rho3-V51* display severe secretion and growth defects in non-permissive conditions, as well as a synthetic lethal phenotype in the double mutant[26].

In this paper, we used a BiFC approach to demonstrate the role of phosphoinositides with stearic acid in optimising the interactions of GTPases with the two exocyst subunits, both using FACS analysis and confocal microscopy. In addition, we also demonstrated a synergistic effect of *psi1*Δ associated with *rho3-V51*, as well as synthetic lethality at intermediate temperatures in the double mutant carrying the *psi1*Δ and *cdc42-6* mutations. These results reflect the disorganisation of Rho GTPase biology in yeast lacking stearic acid in their phosphoinositides. Although GTP hydrolysis of Cdc42p and Rho3p is not required for their role in trafficking[81], we showed that the lack of phosphoinositides with stearic acid in a *psi1*-deficient strain decreased the ratio of GTP/GDP forms for both Rho1p and Rho3p, and perhaps for Cdc42p . This consequently disturbs the role of Sec3p and Exo70p in secretion by decreasing their interaction with their Rho GTPase partners. Hence, the modification of the PI(4,5)P_2 environment modulates the activation state of Rho, disturbing the positioning of these proteins in the membrane, which may influence their ability to interact with the exocyst[12]. These interactions between Rho GTPases and exocyst members take place in their GTP-bound state and should induce an allosteric conformational switch to an activated state[81,82]. The cycle between GTP-state and

GDP-state is regulated by the RhoGEFs and their RhoGAPs partners. Some RhoGEFs (Tus1p, Rom1/2p and Cdc24p) and RhoGAPs (Bem2/3p, Rgd1/2p and Rga1/2p) for Rho1p, Rho3p and Cdc42p, respectively, and the scaffold protein Bem1 for Cdc42p activation, contain specific domains which bind phosphoinositides: PH, F-BAR, PX and basic cluster motifs[14,59,60,62,83-86]. In this way, they may control Rho activity through the action of phosphoinositides.

For the first time, our work demonstrates that the qualitative modification of the acyl chain of phosphoinositides modifies the activity of at least two Rho GTPases involved in the management of exocyst proteins Exo70 and Sec3, consequently controlling the activation of the exocyst and intracellular trafficking. The comparison of architectural modelling of the exocyst complex in wild reference strains[87-89] and in cells lacking stearic acid in their phosphoinositides would be crucial to accurately determine the role of phosphoinositides and Rho GTPases in controlling the assembly and functioning of the exocyst complex.

We speculate that the importance of phosphoinositide acyl chains in the interactions between small G proteins and members of the exocyst may be partially or totally shared by other organisms, specifically in filamentous fungi, plants or mammals. For instance, in *Candida albicans,* pathogenicity is related to its ability to induce hyphae. This morphological switch requires the action of Rho GTPases and a steep gradient of $PI(4,5)P_2$ generated from the tip of the hyphal filament[90–90]. In this pathogenic yeast, CaSec3 and CaExo70 localise at the hyphae tip, spatially separated from a specific structure present during hyphal growth: the Spitzenkörper[91]. Furthermore, previous work showed that plant plasma membrane SEC3, a protein in the pollen tube, is co-localised with PIP2 via its PH domain[41] and can indirectly recruit ROP (Rho Of Plant) GTPases[92,93]. In animal cells, EXOC1 (Sec3) and EXOC7 (Exo70) proteins bind to $PI(4,5)P_2$[40,94,95] and the exocyst complex plays a role mainly during trafficking[40,94,95]. The interactions between Rho-GTPases and the exocyst complex also regulate the transport of Glut4 (the glucose transporter) to the plasma membrane after stimulation by insulin[96]. Phagocytosis requires an interaction between Cdc42 and the exocyst complex[97] and interaction of TC10 with Exo70 is essential for membrane expansion in developing hippocampal neurons and axon regeneration[98].

4 Materials and methods

4.1. Yeast strains and media

The *S. cerevisiae* strains used in this study are listed in Supplementary Table 1. Standard techniques for culturing the yeast were used and the composition of rich (YPD) and synthetic (SC) media for yeast cultures have been reported elsewhere[99]. Yeast strains were usually grown at 30°C, except for thermosensitive mutants when grown at the indicated permissive temperatures.

Double-mutants were generated by inserting a *PSI1* deletion cassette carrying the $G418^R$ marker, or by crossing the conditional *sec* pathway mutants with *psi1*Δ. Double mutants were selected for $G418^R$ and thermosensitivity or cryosensitivity. For crossing with mutants from the Euroscarf collection, double-mutants were isolated from Non-Parental Ditype (NPD) asci.

4.2. Plasmid constructs

For *PSI1* overexpression, a *Bam*HI-*Not*I fragment corresponding to the *PSI1* ORF was inserted under the control of the tetO promoter in pCM189[37]. pRS314-*GFP-PH$^{PLC\delta1}$* dimers were constructed by inserting a *Kpn*I-*Sac*II fragment from pRS406-*2xGFP-PH$^{PLC\delta1}$* [44] into the pRS314 vector[100]. *3xHA-RHO* constructions under the control of the *MET25* promoter were generated using a plasmid derived from pUG36[101], where GFP was replaced by *3xHA*[65]. The bacterial plasmids for the production of GST-C21RBD (rhotekin RBD) and GST-CRIB were generously gifted by Dr Pilar Perez[102] and Dr Robert Arkowitz, respectively[66].

4.3. Yeast strains constructs

Exo70p and Sec3p were tagged at C-terminal part with 6xHA at their chromosomal loci using toolbox [103]. Rho proteins used for OptiPrep™ Floatation Assay were tagged at their N-terminal part with a 6xHA using the pOM13 vector allowing **N-**terminal tagging of proteins expressed by own promoters at their native loci[104]. Strains used for pull-down assay carried plasmid constructs

with *3xHA-RHO* genes transcribed by the *MET25* promoter to conserve a chromosomal allele for *RHO* genes, this is particularly important for strains producing the constitive GTP forms of Rho.

4.4. Determination of cell lethality

After overnight growth, OD_{600} was measured and dead cells were visualised 10 min after mixing 30 µl of culture with 30 µl of methylene blue staining solution. Living cells reduce the dye to a colourless state, but in dead cells the dye stays oxidized and blue. Cell mortality was quantified by the ratio of blue-coloured cells over the total number of cells by counting at least 400 cells[34,105].

4.5. Analysis of phosphoinositide molecular species

Yeast cells were cultured in 100 mL of SC media lacking uracil at 25°C, up to a cell density of 0.5 OD_{600}. Then, the cells were re-inoculated immediately in pre-warmed media and divided into two separate flasks of equal volume: one was maintained for one hour at 25°C (permissive temperature) and the other was shifted to 30°C (intermediate temperature) for one hour. The protocol used was derived from Clark[106] and was described in previous work[13]. Briefly, after lipid extraction, phosphoinositides were extracted and derived with trimethylsilyl-diazomethane (TMS-diazomethane, Sigma-Aldrich, St Louis, MO). Reverse-phase separation was carried out on a Jupiter C4 50×1 mm column using 5 µm particles (Phenomenex) and then molecular species analysis was performed using a mass spectrometer (QTRAP® 5500, ABSciex) coupled to a LC (Liquid Chromatography) system (Ultimate 3000, Dionex).

4.6. Determination of global PIP and PIP2 amounts by [^{14}C] acetate labelling

For logarithmic growth phase labelling, 50 mL samples of both *stt4-4ts* mutants (either overexpressing *PSI1* or not) were grown at 25°C in SC medium lacking uracil and labelled with [1-^{14}C]acetate (1 µCi/mL, specific activity 50.5 Ci/mol) for an additional 15 h of steady-state

lipid labelling (10 generations)[107]. During the log phase, cells were re-inoculated immediately in pre-warmed media and divided into two separate flasks of equal volume: one was maintained for one hour at 25°C (permissive temperature) and the other was shifted to 30°C (intermediate temperature) for one hour. Quantitative analysis of phosphoinositides was carried out according to the method used in a previous paper[13].

4.7. OptiPrep™ Floatation Assay

OptiPrep™ floatation was performed as described previously[108,109] using strains with trafficking landmarks tagged using 6xHA integrated into the native locus. Cells were lysed using glass beads in TNE (50 mM Tris-HCl pH 7.4; 150 mM NaCl; 5 mM EDTA), then the lysate was cleared by centrifugation at 500 *g* for 5 min at 4°C. The cleared lysates were adjusted to 40% OptiPrep™ (Nycomed, Oslo, Norway) with the stock OptiPrep™ solution (60%) to a final volume of 1.35 mL, then deposited at the bottom of 5 mL centrifugation tubes, covered by a 2.16 mL cushion of 30% OptiPrep™ prepared with TNE and 490 µL of TNE. Tubes were centrifuged overnight at 100,000 *g* using a TH660 rotor. Fractions were collected from the top of the gradient and subjected to Western blot analysis.

4.8. Membrane fluidity assessment

Membrane fluidity assessment was determined by Laurdan spectroscopy from intact cells using a protocol described previously[48]. Cells were cultured in YPD media, to an $OD_{600\ nm}$ of 0.4, then 1 ml of each cell culture was pelleted and resuspended at identical concentrations in 1 ml of phosphate buffer, before the addition of Laurdan (prepared in ethanol to a final concentration of 5 µM) and incubation for 1 h at 30°C in the dark. Aliquots of 200 µl of the cells were centrifuged 2 min, resuspended in 50 µl of phosphate buffer and analysed using a CLARIOstar spectrofluorimeter (BMG LABTECH). Fluorescence emission spectra were recorded between 400 nm and 600 nm with excitation at 380 nm. The emission spectrum for each cell sample was corrected by subtraction of the background fluorescence from the unlabelled cell suspension. The

GP value was calculated according to: $GP = \frac{I440-I490}{I440+I490}$, where I_{440} *and* I_{490} represent the fluorescence intensity emitted at 440 nm and 490 nm respectively, as described by Ishmayana[48].

4.9. Fluorescence microscopy

Cells were grown in YPD or SC lacking the appropriate metabolites. Aliquots of exponentially growing yeast cells (0.2 to 0.4 OD_{600} units) were centrifuged, washed once with phosphate-buffered saline solution and the pellet was resuspended in DAKO Fluorescence Mounting Medium (DAKO S3023; 25% [v/v] PBS and 75% [v/v] glycerol). Confocal microscopy was performed using a Zeiss LSM 880 laser microscope (1 Airy pinhole) with a 63× oil objective. The fluorescence of GFP or Venus were observed at 500–600 nm, with the maximum intensities of the emission spectra at 510 and 530 nm respectively, after excitation of the cells with a laser at 488 nm.

4.10. BiFC approaches

Cdc42p, Rho1p and Rho3p were tagged at their N-terminals with VC using a one-step PCR cassette from the pFA6a-His3MX6-p_{CET1}-VC vector[56] integrated using homologous recombination in BY4742 (Mat **α**) and *psi1*Δ (Mat **α**). Exo70p and Sec3p were tagged at their C-terminals with VN using a PCR cassette from the pFA6a-VN-His3MX6 vector and integrated using BY4741 (Mat a) and *psi1*ΔIVc (Mat a). Different combinations were generated by mating haploid and diploid cells with VC and VN tags, selected on SC lacking histidine, lysine and methionine. The BiFC signal was only detected in the growth area for each of the four combinations and scored for quantitative data.

BiFC fluorescence was also quantified by flow cytometry as previously reported[110], using a CyFlow Space (PARTEC). Fluorescence intensity was measured in exponential phase cultures in SC medium, which were then harvested and resuspended in phosphate buffered saline at approximately 50,000 cells per mL. Cells were excited at 488 nm, and fluorescence detected through a 530 nm band pass filter. 50% of the cell population was gated to avoid fluorescence from small molecules.

Some autofluorescence was observed, mainly originating from riboflavin[111]. This was measured in both the *psi1*Δ background and the control strain without Venus and subtracted from the fluorescence intensities detected for each diploid strain comprising the two domains (VC and VN) of the fluorochrome. Calibration was performed by measuring the fluorescence intensity signal for 20,000 cells.

4.11. RT-qPCR

A RNeasy-PlusMini Kit (Qiagen) was used for RNA purification. rDNase I was used to remove contaminating DNA (DNA-Free Kit; Invitrogen), and cDNA was obtained using a SuperScript™ II Reverse Transcriptase kit (Invitrogen). Real-time quantitative PCR reactions were performed in a CFX96 Real-Time System (Bio-Rad) using the GoTaq qPCR Master mix (Promega). The software CFX Manager (v.3.1; Bio-Rad) was used for data acquisition and analysis. The Ct method was used to normalise transcript abundance with the references mRNA *ALG9* (Mannosyltransferase), *TAF10* (TFIID and SAGA complexes), and *UBC6* (Ubiquitin-conjugating) validated for optimal quantitative expression analysis [112].

4.12. Determination of Rho activation by Rho-GTP pull-down assay

The degree of Rho activation was determined *in vivo* by the amount of GTP-bound Rho, revealed by a pull-down assay performed according to a previously described protocol[65]. The wild-type and *psi1*Δ strains were each transformed with one of pU009-*3xHA-RHO1*, pU009-*3xHA-RHO3* or pU009-*3xHA-CDC42*, producing the wild-type 3xHA-Rho1p, 3xHA-Rho3p and 3xHA-Cdc42p strains, respectively. The wild-type strain was also transformed with one or other of the plasmids pU009-*3xHA-RHO1*^{Q68L}*-GTP*, pU009-*3xHA-RHO3*^{Q74L}*-GTP* or pU009-*3xHA-CDC42*^{Q61L}*-GTP*, expressing constitutively activated Rho1p, Rho3p and Cdc42p.

Cells were cultured in SC lacking uracil up to a density of 0.4 OD_{600nm}, then moved into prewarmed SC lacking uracil and methionine and grown up to a density of approximately 2 OD_{600nm} before harvesting and lysing the cells using glass beads as described previously[65]. Then, GTP-bound Rho1p and Rho3p were pulled down from the cell extracts by binding to GST-C21RBD (rhotekin RBD), previously obtained and purified from *E. coli*[64,65]. Cdc42-GTP was pulled down using the CRIB domain from the Ste20 protein[66]. Anti-HA 12CA5 monoclonal

antibodies were used for Western blot analysis. The amount of GTP-bound Rho pulled down compared to total Rho levels for each sample was based on band intensity quantification. Densitometric analysis was performed using the free ImageJ software after BIO-RAD ChemiDoc™ acquisitions. Pgk1p was used as a loading control for total Rho and was measured using an anti-Pgk1 monoclonal antibody 22C5D8 (Thermo Fisher Scientific). GST-CRIB or GST-RDB were quantified after staining the blotted membranes with Red Ponceau[64].

ACKNOWLEDGEMENTS

The heat-sensitive strains AAY104, SEY6210 and AAY202 were generously provided by Chris Stefan (University of California, San Diego) and strain CTY1568 was obtained from Dr Vytas Bankaitis. We thank Dr Randy Schekman for the gift of the *sec* mutants, Dr Patrick Bernnwald for *cdc42-6* and *rho3-V51*, Dr Wei Guo for SEC3-GFP and EXO70-GFP, Dr Isabelle Sagot for the gift of the vectors for BiFC and for helpful discussions, Dr Derek McCusker for the gift of the GFP-CDC42 construction, Dr Tim Levine for the plasmids with biosensors to visualise PI(4,5)P_2 *in vivo*, Dr Robert Arkowitz for the gift of the plasmid carrying the CRIB domain from Ste20p and Dr Pilar Perez for the plasmid producing rhotekin RBD. Lipidomic analyses were performed at the Toulouse INSERM Metatoul-Lipidomique and at Bordeaux Metabolome Facility-MetaboHUB (ANR-INBS-0011). Imaging was performed at the Bordeaux Imaging Center, part of the France BioImaging national infrastructure, with technical help from Brigitte Batailler and Lysiane Brocard. FACS analyses were performed with the help of Dr Catherine Cheniclet.

All authors declare that there is no conflict of interest

1. Pruyne D, Legesse-Miller A, Gao L, Dong Y, Bretscher A. Mechanisms of polarized growth and organelle segregation in yeast. *Annu Rev Cell Dev Biol.* 2004;20:559-591.
2. Mizuno-Yamasaki E, Rivera-Molina F, Novick P. GTPase networks in membrane traffic. *Annu Rev Biochem.* 2012;81:637-659.
3. Wu B, Guo W. The Exocyst at a Glance. *J Cell Sci.* 2015;128(16):2957-2964.
4. Yakir-Tamang L, Gerst JE. Phosphoinositides, exocytosis and polarity in yeast: all about actin? *Trends Cell Biol.* 2009;19(12):677-684.
5. Johansen J, Ramanathan V, Beh CT. Vesicle trafficking from a lipid perspective: Lipid regulation of exocytosis in Saccharomyces cerevisiae. *Cell Logist.* 2012;2(3):151-160.
6. Mizuno-Yamasaki E, Medkova M, Coleman J, Novick P. Phosphatidylinositol 4-phosphate controls both membrane recruitment and a regulatory switch of the Rab GEF Sec2p. *Dev Cell.* 2010;18(5):828-840.
7. Yakir-Tamang L, Gerst JE. A phosphatidylinositol-transfer protein and phosphatidylinositol-4-phosphate 5-kinase control Cdc42 to regulate the actin cytoskeleton and secretory pathway in yeast. *Mol Biol Cell.* 2009;20(15):3583-3597.
8. Audhya A, Foti M, Emr SD. Distinct roles for the yeast phosphatidylinositol 4-kinases, Stt4p and Pik1p, in secretion, cell growth, and organelle membrane dynamics. *Mol Biol Cell.* 2000;11(8):2673-2689.
9. Boyd C, Hughes T, Pypaert M, Novick P. Vesicles carry most exocyst subunits to exocytic sites marked by the remaining two subunits, Sec3p and Exo70p. *J Cell Biol.* 2004;167(5):889-901.
10. He B, Guo W. The exocyst complex in polarized exocytosis. *Curr Opin Cell Biol.* 2009;21(4):537-542.
11. Martin TF. PI(4,5)P(2)-binding effector proteins for vesicle exocytosis. *Biochim Biophys Acta.* 2014;1851(6):785-793.
12. Pleskot R, Cwiklik L, Jungwirth P, Zarsky V, Potocky M. Membrane targeting of the yeast exocyst complex. *Biochim Biophys Acta.* 2015;1848(7):1481-1489.
13. Doignon F, Laquel P, Testet E, Tuphile K, Fouillen L, Bessoule JJ. Requirement of phosphoinositides containing stearic acid to control cell polarity. *Mol Cell Biol.* 2016;36(5):765-780.
14. Meca J, Massoni-Laporte A, Martinez D, et al. Avidity-driven polarity establishment via multivalent lipid-GTPase module interactions. *EMBO J.* 2018;38(3).
15. Reithinger JH, Kim JE, Kim H. Sec62 protein mediates membrane insertion and orientation of moderately hydrophobic signal anchor proteins in the endoplasmic reticulum (ER). *J Biol Chem.* 2013;288(25):18058-18067.
16. Rothblatt JA, Deshaies RJ, Sanders SL, Daum G, Schekman R. Multiple genes are required for proper insertion of secretory proteins into the endoplasmic reticulum in yeast. *J Cell Biol.* 1989;109(6 Pt 1):2641-2652.
17. Bohni PC, Deshaies RJ, Schekman RW. SEC11 is required for signal peptide processing and yeast cell growth. *J Cell Biol.* 1988;106(4):1035-1042.
18. McMahon C, Studer SM, Clendinen C, Dann GP, Jeffrey PD, Hughson FM. The structure of Sec12 implicates potassium ion coordination in Sar1 activation. *J Biol Chem.* 2012;287(52):43599-43606.
19. Kaiser CA, Schekman R. Distinct sets of SEC genes govern transport vesicle formation and fusion early in the secretory pathway. *Cell.* 1990;61(4):723-733.

20. Richardson BC, McDonold CM, Fromme JC. The Sec7 Arf-GEF is recruited to the trans-Golgi network by positive feedback. *Dev Cell.* 2012;22(4):799-810.
21. Novick P, Field C, Schekman R. Identification of 23 complementation groups required for post-translational events in the yeast secretory pathway. *Cell.* 1980;21(1):205-215.
22. Adnan M, Islam W, Zhang J, Zheng W, Lu GD. Diverse Role of SNARE Protein Sec22 in Vesicle Trafficking, Membrane Fusion, and Autophagy. *Cells.* 2019;8(4).
23. Flanagan JJ, Mukherjee I, Barlowe C. Examination of Sec22 Homodimer Formation and Role in SNARE-dependent Membrane Fusion. *J Biol Chem.* 2015;290(17):10657-10666.
24. Curwin AJ, Leblanc MA, Fairn GD, McMaster CR. Localization of lipid raft proteins to the plasma membrane is a major function of the phospholipid transfer protein Sec14. *PLoS One.* 2013;8(1):e55388.
25. Bankaitis VA, Malehorn DE, Emr SD, Greene R. The Saccharomyces cerevisiae SEC14 gene encodes a cytosolic factor that is required for transport of secretory proteins from the yeast Golgi complex. *J Cell Biol.* 1989;108(4):1271-1281.
26. Adamo JE, Moskow JJ, Gladfelter AS, Viterbo D, Lew DJ, Brennwald PJ. Yeast Cdc42 functions at a late step in exocytosis, specifically during polarized growth of the emerging bud. *J Cell Biol.* 2001;155(4):581-592.
27. Songer JA, Munson M. Sec6p anchors the assembled exocyst complex at sites of secretion. *Mol Biol Cell.* 2009;20(3):973-982.
28. Adamo JE, Rossi G, Brennwald P. The Rho GTPase Rho3 has a direct role in exocytosis that is distinct from its role in actin polarity. *Mol Biol Cell.* 1999;10(12):4121-4133.
29. Parlati F, McNew JA, Fukuda R, Miller R, Sollner TH, Rothman JE. Topological restriction of SNARE-dependent membrane fusion. *Nature.* 2000;407(6801):194-198.
30. Eisfeld K, Riffer F, Mentges J, Schmitt MJ. Endocytotic uptake and retrograde transport of a virally encoded killer toxin in yeast. *Mol Microbiol.* 2000;37(4):926-940.
31. Benedetti H, Raths S, Crausaz F, Riezman H. The END3 gene encodes a protein that is required for the internalization step of endocytosis and for actin cytoskeleton organization in yeast. *Mol Biol Cell.* 1994;5(9):1023-1037.
32. Kaksonen M, Toret CP, Drubin DG. A modular design for the clathrin- and actin-mediated endocytosis machinery. *Cell.* 2005;123(2):305-320.
33. Daboussi L, Costaguta G, Payne GS. Phosphoinositide-mediated clathrin adaptor progression at the trans-Golgi network. *Nat Cell Biol.* 2012;14(3):239-248.
34. de Bettignies G, Barthe C, Morel C, Peypouquet MF, Doignon F, Crouzet M. RGD1 genetically interacts with MID2 and SLG1, encoding two putative sensors for cell integrity signalling in Saccharomyces cerevisiae. *Yeast.* 1999;15(16):1719-1731.
35. Adams AE, Johnson DI, Longnecker RM, Sloat BF, Pringle JR. CDC42 and CDC43, two additional genes involved in budding and the establishment of cell polarity in the yeast Saccharomyces cerevisiae. *J Cell Biol.* 1990;111(1):131-142.
36. Dong Y, Pruyne D, Bretscher A. Formin-dependent actin assembly is regulated by distinct modes of Rho signaling in yeast. *J Cell Biol.* 2003;161(6):1081-1092.
37. Gari E, Piedrafita L, Aldea M, Herrero E. A set of vectors with a tetracycline-regulatable promoter system for modulated gene expression in Saccharomyces cerevisiae. *Yeast.* 1997;13(9):837-848.
38. Routt SM, Ryan MM, Tyeryar K, et al. Nonclassical PITPs activate PLD via the Stt4p PtdIns-4-kinase and modulate function of late stages of exocytosis in vegetative yeast. *Traffic.* 2005;6(12):1157-1172.

39. He B, Xi F, Zhang X, Zhang J, Guo W. Exo70 interacts with phospholipids and mediates the targeting of the exocyst to the plasma membrane. *EMBO J.* 2007;26(18):4053-4065.
40. Liu J, Zuo X, Yue P, Guo W. Phosphatidylinositol 4,5-bisphosphate mediates the targeting of the exocyst to the plasma membrane for exocytosis in mammalian cells. *Mol Biol Cell.* 2007;18(11):4483-4492.
41. Bloch D, Pleskot R, Pejchar P, et al. Exocyst SEC3 and Phosphoinositides Define Sites of Exocytosis in Pollen Tube Initiation and Growth. *Plant Physiol.* 2016;172(2):980-1002.
42. D'Angelo G, Vicinanza M, Di Campli A, De Matteis MA. The multiple roles of PtdIns(4)P -- not just the precursor of PtdIns(4,5)P2. *J Cell Sci.* 2008;121(Pt 12):1955-1963.
43. Stefan CJ, Audhya A, Emr SD. The yeast synaptojanin-like proteins control the cellular distribution of phosphatidylinositol (4,5)-bisphosphate. *Mol Biol Cell.* 2002;13(2):542-557.
44. Levine TP, Munro S. Targeting of Golgi-specific pleckstrin homology domains involves both PtdIns 4-kinase-dependent and -independent components. *Curr Biol.* 2002;12(9):695-704.
45. Zhang X, Orlando K, He B, et al. Membrane association and functional regulation of Sec3 by phospholipids and Cdc42. *J Cell Biol.* 2008;180(1):145-158.
46. Liu D, Li X, Shen D, Novick P. Two subunits of the exocyst, Sec3p and Exo70p, can function exclusively on the plasma membrane. *Mol Biol Cell.* 2018;29(6):736-750.
47. Tuller G, Nemec T, Hrastnik C, Daum G. Lipid composition of subcellular membranes of an FY1679-derived haploid yeast wild-type strain grown on different carbon sources. *Yeast.* 1999;15(14):1555-1564.
48. Ishmayana S, Kennedy UJ, Learmonth RP. Further investigation of relationships between membrane fluidity and ethanol tolerance in Saccharomyces cerevisiae. *World J Microbiol Biotechnol.* 2017;33(12):218.
49. Owen DM, Rentero C, Magenau A, Abu-Siniyeh A, Gaus K. Quantitative imaging of membrane lipid order in cells and organisms. *Nat Protoc.* 2012;7(1):24-35.
50. Amaro M, Reina F, Hof M, Eggeling C, Sezgin E. Laurdan and Di-4-ANEPPDHQ probe different properties of the membrane. *J Phys D Appl Phys.* 2017;50(13):134004.
51. Klose C, Ejsing CS, Garcia-Saez AJ, et al. Yeast lipids can phase-separate into micrometer-scale membrane domains. *J Biol Chem.* 2010;285(39):30224-30232.
52. Robinson NG, Guo L, Imai J, Toh EA, Matsui Y, Tamanoi F. Rho3 of Saccharomyces cerevisiae, which regulates the actin cytoskeleton and exocytosis, is a GTPase which interacts with Myo2 and Exo70. *Mol Cell Biol.* 1999;19(5):3580-3587.
53. Guo W, Tamanoi F, Novick P. Spatial regulation of the exocyst complex by Rho1 GTPase. *Nat Cell Biol.* 2001;3(4):353-360.
54. Wu H, Turner C, Gardner J, Temple B, Brennwald P. The Exo70 subunit of the exocyst is an effector for both Cdc42 and Rho3 function in polarized exocytosis. *Mol Biol Cell.* 2010;21(3):430-442.
55. Finger FP, Hughes TE, Novick P. Sec3p is a spatial landmark for polarized secretion in budding yeast. *Cell.* 1998;92(4):559-571.
56. Sung MK, Huh WK. Bimolecular fluorescence complementation analysis system for in vivo detection of protein-protein interaction in Saccharomyces cerevisiae. *Yeast.* 2007;24(9):767-775.

57. Wu H, Brennwald P. The function of two Rho family GTPases is determined by distinct patterns of cell surface localization. *Mol Cell Biol.* 2010;30(21):5207-5217.
58. Zhang X, Bi E, Novick P, et al. Cdc42 interacts with the exocyst and regulates polarized secretion. *J Biol Chem.* 2001;276(50):46745-46750.
59. Mukherjee D, Sen A, Boettner DR, et al. Bem3, a Cdc42 GTPase-activating protein, traffics to an intracellular compartment and recruits the secretory Rab GTPase Sec4 to endomembranes. *J Cell Sci.* 2013;126(Pt 20):4560-4571.
60. Saito K, Fujimura-Kamada K, Hanamatsu H, et al. Transbilayer phospholipid flipping regulates Cdc42p signaling during polarized cell growth via Rga GTPase-activating proteins. *Dev Cell.* 2007;13(5):743-751.
61. Manning BD, Padmanabha R, Snyder M. The Rho-GEF Rom2p localizes to sites of polarized cell growth and participates in cytoskeletal functions in Saccharomyces cerevisiae. *Mol Biol Cell.* 1997;8(10):1829-1844.
62. Prouzet-Mauleon V, Lefebvre F, Thoraval D, Crouzet M, Doignon F. Phosphoinositides affect both the cellular distribution and activity of the F-BAR-containing RhoGAP Rgd1p in yeast. *J Biol Chem.* 2008;283(48):33249-33257.
63. Lefebvre F, Prouzet-Mauleon V, Hugues M, et al. Secretory pathway-dependent localization of the Saccharomyces cerevisiae Rho GTPase-activating protein Rgd1p at growth sites. *Eukaryot Cell.* 2012;11(5):590-600.
64. Onishi M, Pringle JR. Analysis of Rho-GTPase Activity During Budding Yeast Cytokinesis. *Methods Mol Biol.* 2016;1369:205-218.
65. Claret S, Roumanie O, Prouzet-Mauleon V, et al. Evidence for functional links between the Rgd1-Rho3 RhoGAP-GTPase module and Tos2, a protein involved in polarized growth in Saccharomyces cerevisiae. *FEMS Yeast Res.* 2011;11(2):179-191.
66. Barale S, McCusker D, Arkowitz RA. Cdc42p GDP/GTP cycling is necessary for efficient cell fusion during yeast mating. *Mol Biol Cell.* 2006;17(6):2824-2838.
67. Prigent M, Boy-Marcotte E, Chesneau L, et al. The RabGAP proteins Gyp5p and Gyl1p recruit the BAR domain protein Rvs167p for polarized exocytosis. *Traffic.* 2011;12(8):1084-1097.
68. Guo W, Novick P. The exocyst meets the translocon: a regulatory circuit for secretion and protein synthesis? *Trends Cell Biol.* 2004;14(2):61-63.
69. Toikkanen JH, Miller KJ, SÃ¶derlund H, JÃ¤ntti J, KerÃ¤nen S. The Î² Subunit of the Sec61p Endoplasmic Reticulum Translocon Interacts with the Exocyst Complex in Saccharomyces cerevisiae. *Journal of Biological Chemistry.* 2003;278(23):20946-20953.
70. Imae R, Inoue T, Kimura M, et al. Intracellular phospholipase A1 and acyltransferase, which are involved in Caenorhabditis elegans stem cell divisions, determine the sn-1 fatty acyl chain of phosphatidylinositol. *Mol Biol Cell.* 2010;21(18):3114-3124.
71. Gloor Y, Schone M, Habermann B, et al. Interaction between Sec7p and Pik1p: the first clue for the regulation of a coincidence detection signal. *Eur J Cell Biol.* 2010;89(8):575-583.
72. Wera S, Bergsma JC, Thevelein JM. Phosphoinositides in yeast: genetically tractable signalling. *FEMS Yeast Res.* 2001;1(1):9-13.
73. Wild AC, Yu JW, Lemmon MA, Blumer KJ. The p21-activated protein kinase-related kinase Cla4 is a coincidence detector of signaling by Cdc42 and phosphatidylinositol 4-phosphate. *J Biol Chem.* 2004;279(17):17101-17110.

74. Versele M, Thorner J. Septin collar formation in budding yeast requires GTP binding and direct phosphorylation by the PAK, Cla4. *J Cell Biol.* 2004;164(5):701-715.
75. Strahl T, Thorner J. Synthesis and function of membrane phosphoinositides in budding yeast, Saccharomyces cerevisiae. *Biochim Biophys Acta.* 2007;1771(3):353-404.
76. Garrenton LS, Stefan CJ, McMurray MA, Emr SD, Thorner J. Pheromone-induced anisotropy in yeast plasma membrane phosphatidylinositol-4,5-bisphosphate distribution is required for MAPK signaling. *Proc Natl Acad Sci U S A.* 2010;107(26):11805-11810.
77. Nakatsu F, Baskin JM, Chung J, et al. PtdIns4P synthesis by PI4KIIIalpha at the plasma membrane and its impact on plasma membrane identity. *J Cell Biol.* 2012;199(6):1003-1016.
78. Rapali P, Mitteau R, Braun C, et al. Scaffold-mediated gating of Cdc42 signalling flux. *Elife.* 2017;6.
79. Yoshida S, Bartolini S, Pellman D. Mechanisms for concentrating Rho1 during cytokinesis. *Genes Dev.* 2009;23(7):810-823.
80. Sartorel E, Unlu C, Jose M, et al. Phosphatidylserine and GTPase activation control Cdc42 nanoclustering to counter dissipative diffusion. *Mol Biol Cell.* 2018;29(11):1299-1310.
81. Roumanie O, Wu H, Molk JN, Rossi G, Bloom K, Brennwald P. Rho GTPase regulation of exocytosis in yeast is independent of GTP hydrolysis and polarization of the exocyst complex. *J Cell Biol.* 2005;170(4):583-594.
82. Rossi G, Lepore D, Kenner L, et al. Exocyst structural changes associated with activation of tethering downstream of Rho/Cdc42 GTPases. *J Cell Biol.* 2020;219(2).
83. Schmelzle T, Helliwell SB, Hall MN. Yeast protein kinases and the RHO1 exchange factor TUS1 are novel components of the cell integrity pathway in yeast. *Mol Cell Biol.* 2002;22(5):1329-1339.
84. Ozaki K, Tanaka K, Imamura H, et al. Rom1p and Rom2p are GDP/GTP exchange proteins (GEPs) for the Rho1p small GTP binding protein in Saccharomyces cerevisiae. *EMBO J.* 1996;15(9):2196-2207.
85. Roumanie O, Weinachter C, Larrieu I, Crouzet M, Doignon F. Functional characterization of the Bag7, Lrg1 and Rgd2 RhoGAP proteins from Saccharomyces cerevisiae. *FEBS Lett.* 2001;506(2):149-156.
86. Martinez D, Langlois d'Estaintot B, Granier T, et al. Structural evidence of a phosphoinositide-binding site in the Rgd1-RhoGAP domain. *Biochem J.* 2017;474(19):3307-3319.
87. Mei K, Li Y, Wang S, et al. Cryo-EM structure of the exocyst complex. *Nat Struct Mol Biol.* 2018;25(2):139-146.
88. Heider MR, Gu M, Duffy CM, et al. Subunit connectivity, assembly determinants and architecture of the yeast exocyst complex. *Nat Struct Mol Biol.* 2016;23(1):59-66.
89. Donovan KW, Bretscher A. Tracking individual secretory vesicles during exocytosis reveals an ordered and regulated process. *J Cell Biol.* 2015;210(2):181-189.
90. Corvest V, Bogliolo S, Follette P, Arkowitz RA, Bassilana M. Spatiotemporal regulation of Rho1 and Cdc42 activity during Candida albicans filamentous growth. *Mol Microbiol.* 2013;89(4):626-648.
91. Jones LA, Sudbery PE. Spitzenkorper, exocyst, and polarisome components in Candida albicans hyphae show different patterns of localization and have distinct dynamic properties. *Eukaryot Cell.* 2010;9(10):1455-1465.

92. Guan Y, Guo J, Li H, Yang Z. Signaling in pollen tube growth: crosstalk, feedback, and missing links. *Mol Plant.* 2013;6(4):1053-1064.
93. Lavy M, Bloch D, Hazak O, et al. A Novel ROP/RAC effector links cell polarity, root-meristem maintenance, and vesicle trafficking. *Curr Biol.* 2007;17(11):947-952.
94. Li Q, Li N, Liu CY, et al. Ezrin/Exocyst complex regulates mucin 5AC secretion induced by neutrophil elastase in human airway epithelial cells. *Cell Physiol Biochem.* 2015;35(1):326-338.
95. Xiong X, Xu Q, Huang Y, et al. An association between type Igamma PI4P 5-kinase and Exo70 directs E-cadherin clustering and epithelial polarization. *Mol Biol Cell.* 2012;23(1):87-98.
96. Inoue M, Chang L, Hwang J, Chiang SH, Saltiel AR. The exocyst complex is required for targeting of Glut4 to the plasma membrane by insulin. *Nature.* 2003;422(6932):629-633.
97. Mohammadi S, Isberg RR. Cdc42 interacts with the exocyst complex to promote phagocytosis. *J Cell Biol.* 2013;200(1):81-93.
98. Dupraz S, Grassi D, Bernis ME, et al. The TC10-Exo70 complex is essential for membrane expansion and axonal specification in developing neurons. *J Neurosci.* 2009;29(42):13292-13301.
99. Rose MD, Winston F, Hieter P. *Methods in Yeast Genetics: A Laboratory Course Manual.* Cold Spring Harbor, New York: Cold Spring Harbor Laboratory Press; 1990.
100. Sikorski RS, Hieter P. A system of shuttle vectors and yeast host strains designed for efficient manipulation of DNA in Saccharomyces cerevisiae. *Genetics.* 1989;122(1):19-27.
101. Niedenthal RK, Riles L, Johnston M, Hegemann JH. Green fluorescent protein as a marker for gene expression and subcellular localization in budding yeast. *Yeast.* 1996;12(8):773-786.
102. Calonge TM, Arellano M, Coll PM, Perez P. Rga5p is a specific Rho1p GTPase-activating protein that regulates cell integrity in Schizosaccharomyces pombe. *Mol Microbiol.* 2003;47(2):507-518.
103. Janke C, Magiera MM, Rathfelder N, et al. A versatile toolbox for PCR-based tagging of yeast genes: new fluorescent proteins, more markers and promoter substitution cassettes. *Yeast.* 2004;21(11):947-962.
104. Gauss R, Trautwein M, Sommer T, Spang A. New modules for the repeated internal and N-terminal epitope tagging of genes in Saccharomyces cerevisiae. *Yeast.* 2005;22(1):1-12.
105. Rose AH. Growth and handling of yeasts. *Methods Cell Biol.* 1975;12:1-16.
106. Clark J, Anderson KE, Juvin V, et al. Quantification of PtdInsP3 molecular species in cells and tissues by mass spectrometry. *Nat Methods.* 2011;8(3):267-272.
107. Gaspar ML, Aregullin MA, Jesch SA, Henry SA. Inositol induces a profound alteration in the pattern and rate of synthesis and turnover of membrane lipids in Saccharomyces cerevisiae. *J Biol Chem.* 2006;281(32):22773-22785.
108. Bagnat M, Keranen S, Shevchenko A, Simons K. Lipid rafts function in biosynthetic delivery of proteins to the cell surface in yeast. *Proc Natl Acad Sci U S A.* 2000;97(7):3254-3259.
109. Aronova S, Wedaman K, Anderson S, Yates J, 3rd, Powers T. Probing the membrane environment of the TOR kinases reveals functional interactions between TORC1, actin,

and membrane trafficking in Saccharomyces cerevisiae. *Mol Biol Cell.* 2007;18(8):2779-2794.
110. Sung MK, Huh WK. In vivo quantification of protein-protein interactions in Saccharomyces cerevisiae using bimolecular fluorescence complementation assay. *J Microbiol Methods.* 2010;83(2):194-201.
111. Maslanka R, Kwolek-Mirek M, Zadrag-Tecza R. Autofluorescence of yeast Saccharomyces cerevisiae cells caused by glucose metabolism products and its methodological implications. *J Microbiol Methods.* 2018;146:55-60.
112. Teste MA, Duquenne M, Francois JM, Parrou JL. Validation of reference genes for quantitative expression analysis by real-time RT-PCR in Saccharomyces cerevisiae. *BMC Mol Biol.* 2009;10:99.

FIGURE 1 Deletion of *PSI1* shows genetic interactions with some mutants involved in secretory pathway.

Exponentially growing cells of the mentioned genotype were suspended in YPD medium and tenfold serial dilutions were spotted on YPD plates and were incubated at (A) 25°C (permissive temperature), (B) 30°C (intermediate temperature), and (C) 37°C (restrictive temperature) for 24 hours.

FIGURE 2 *PSI1* constitutive overexpression suppresses growth defect of *cdc42-6* mutant.

Cells in the exponential growth phase grown at 25°C from *cdc42-6* mutant strain or BY647 control strain transformed with the empty vector or overexpressing the *PSI1* gene were suspended in SC minus uracil medium and tenfold serial dilution were spotted on SC minus uracil plates and incubated at 25°C (permissive temperature), and 30°C (intermediate temperature) for 2 days.

FIGURE 3 *PSI1* constitutive overexpression suppresses the growth defect of the *stt4-4ts* mutant. Exponentially growing cells with the empty vector (pCM189) or constitutively overexpressing *PSI1* (pCM189 + *PSI1*) were suspended in SC minus uracil medium and diluted two times by a factor of 10. These serial dilutions were spotted on SC minus uracil plates and incubated at 25°C (permissive temperature), 30°C (intermediate temperature) and 37°C (restrictive temperature) for 2 days.

FIGURE 4 *PSI1* constitutive overexpression suppresses the growth defect of the *stt4-4ts* mutant by the relocation of $PI(4,5)P_2$ to the growth area.

(A) SEY6210 and *stt4-4ts* strains producing GFP-$PH^{PLC\delta1}$ dimer (biosensor of $PI(4,5)P_2$) and overexpressing *PSI1* or not, were cultured in SC minus uracil and tryptophan to mid-log phase at 25°C (permissive temperature), then shifted at 30°C for 1 hour. After harvest, cells were observed by confocal microscopy and the fluorescence of $PI(4,5)P_2$ biosensor observed at the growth area. Bars, 5 μm. (B) Cells with fluorescence at the growth area were scored (N>300, 3 independent experiments). An unpaired, two-tailed *t*-test was used: **p*<0.05; ***p*<0.01. (C) Ratio of fluorescence intensity at growth area compared to mother cells. The calculations of these ratios were performed by selecting equal areas of the plasma membrane from the bud region (tip or neck) or from the mother cell body. Quantification of the pixels was performed using image J software. An unpaired, two-tailed *t*-test was used: ***p*<0.01; ****p*<0.001.

FIGURE 5 Effect of *PSI1* constitutive overexpression in *stt4-4ts* mutant, on the molecular fatty acid composition of (A) PI, (B) PIP, (C) PIP2; or in the control SEY6210 (D) PI, (E) PIP, (F) PIP2

Cells were cultured in SC medium without uracil at 25°C up to early log-phase. The cells were re-inoculated immediately in pre-warmed media and divided into two separated flasks of equal volume: one was maintained 1 hour at 25°C (permissive temperature) and the other was shifted at 30°C (intermediate temperature) for 1 hour. Cells were harvested and lipids were extracted and quantified by RP-LC-MS/MS.

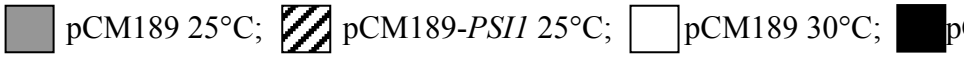 pCM189 25°C; pCM189-*PSI1* 25°C; pCM189 30°C; pCM189-*PSI1* 30°C

Data are means from triplicate measurements. An unpaired, two-tailed *t*-test was used: **p*<0.05; ***p*<0.01; ****p*<0.001.

FIGURE 6 Specific cell polarity landmarks change their membrane environment in cell deficient for phosphoinositides containing stearic acid.

Cell extracts of different diploid strains producing either of the landmarks tagged with 6xHA in wild-type and *psi1*Δ genetic background, were subjected to 0-40% density OptiPrep™ gradients as described in the Material & Methods section. Fractions collected from the top of the gradient were analysed by western blotting using anti HA 12CA5 monoclonal antibody.

FIGURE 7 The specific interactions between Rho GTPases and subunits of the exocyst are dramatically disturbed by a lack of phosphoinositides with stearic acid.

Specific interactions between Rho proteins and exocyst components were analyzed based on Bimolecular Fluorescence Complementation Assay (BiFC) and scored after flow cytometry and confocal microscopy analysis.

(A) Quantitative BiFC Flow cytometry measurements. Cells were harvested and diluted at a final concentration of 50,000 cells/ml in PBS buffer and excited at 488 nm. The emission of cells fluorescence is detected through a 530 nm band pass filter, and 50% of the cell population was gated to subtract the fluorescence signal from small molecules. The measurements were standardized by accumulating the fluorescence signal after 20,000 events (i.e. 20,000 isolated cells passed one by one in the cytometer cell). Cells cultures were analysed at least 3 times per session. The background noise of the autofluorescence of the cells without fluorochrome Venus was determined for the mutant *psi1*Δ and wild type control cells and subtracted from the fluorescence signal of each of the two strains with the fluorochrome. Results were the compilation of 5 sessions for statistical analysis: two-tailed *t*-tests which showed a P values **p<0.01; ***p<0.001.

(B) Confocal microscopy analysis of the specific BiFC signal at growing sites of cells. Cells grown to log phase in YPD at 30°C were analysed and scored for Venus fluorescence by LSM880 confocal microscopy. Cells displayed a specific BiFC fluorescence signal only at their growth area (mostly small buds and bud necks), meaning that Rho GTPases and Exocyst interactions are efficient. Comparisons of the proportion of cells with a polarised BiFC signal for each case of reconstituted fluorochrome between WT and *psi1*Δ/*psi1*Δ were done using

unpaired, two-tailed *t*-tests which showed a P values *p<0.05; **p<0.01; (N >300, three independent experiments).

FIGURE 8 The lack of stearic acid in phosphoinositides greatly reduces the activation level of the GTP-bound Rho GTPases which control the exocyst.

(A) Western blot analysis of the activated Rho1, Rho3 and Cdc42 proteins by Pull Down assays. Rho1-GTP and Rho3-GTP were pulled-down with GST-RBD of human Rhotekin; and Cdc42-GTP with GST-CRIB of Ste20p, from BY4742 wild-type or *psi1*Δ cells extracts overexpressing constitutively WT allelic forms of the HA tagged Rho proteins or overexpressing constitutively their HA tagged GTP-blocked forms in the WT background. GST-Rho were revealed using anti-HA 12CA5 monoclonal antibody, Pgk1p was used as loading control for total Rho, and identified by a specific anti-Pgk1 antibody. The intensities of the activated pulled down GTP forms of Rho1p, Rho3p and Cdc42p are reduced in the *psi1*Δ mutant compared to the control strain. The molecular weight of each of the proteins were the following: 3xHA-Rho1p: 27.5 kDa; 3xHA-Rho3p: 29.7 kDa; 3xHA Cdc42p: 25.7 kDa; GST-CRIB (Ste20): 31 kDa; GST-RDB (Rhotekin): 36 kDa; Pgk1p: 50 kDa.

(B) Quantitative analysis of the GTP-bound forms for Rho1p, Rho3p and Cdc42p in the different background based on pull-down assays. The amounts of pulled-down GTP-Rho relative to the total Rho levels were determined for each strain and ratios were normalised to the control performed with BY4742. The results were the compilation of 3 sessions for statistical analysis: two-tailed *t*-tests which showed a P values **p<0.01; ***p<0.001.

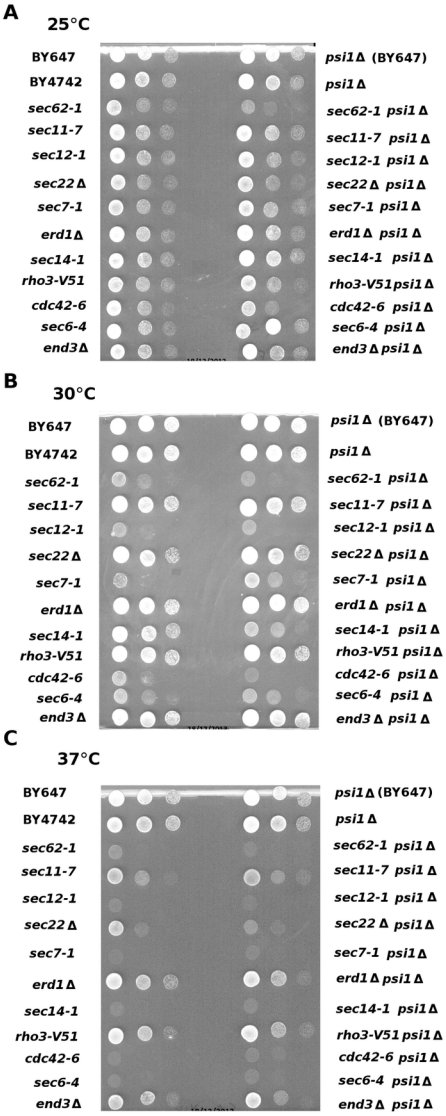

TRA_12829_Fig 1.tif

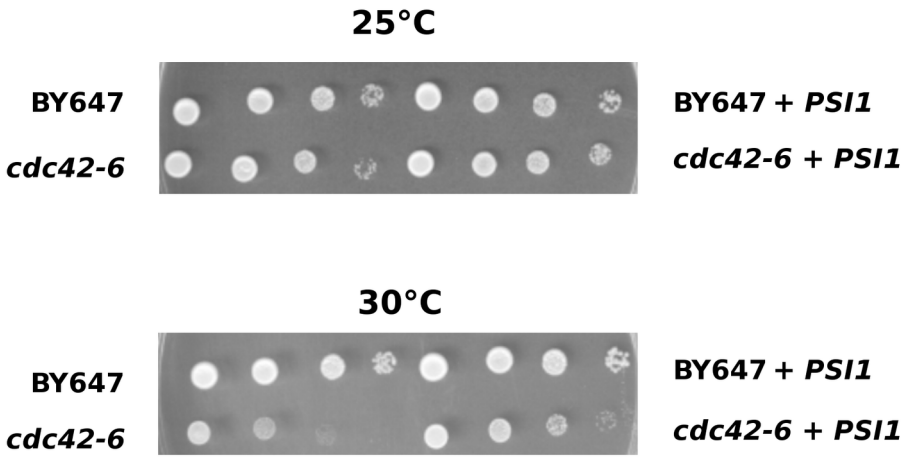

TRA_12829_Fig 2.tif

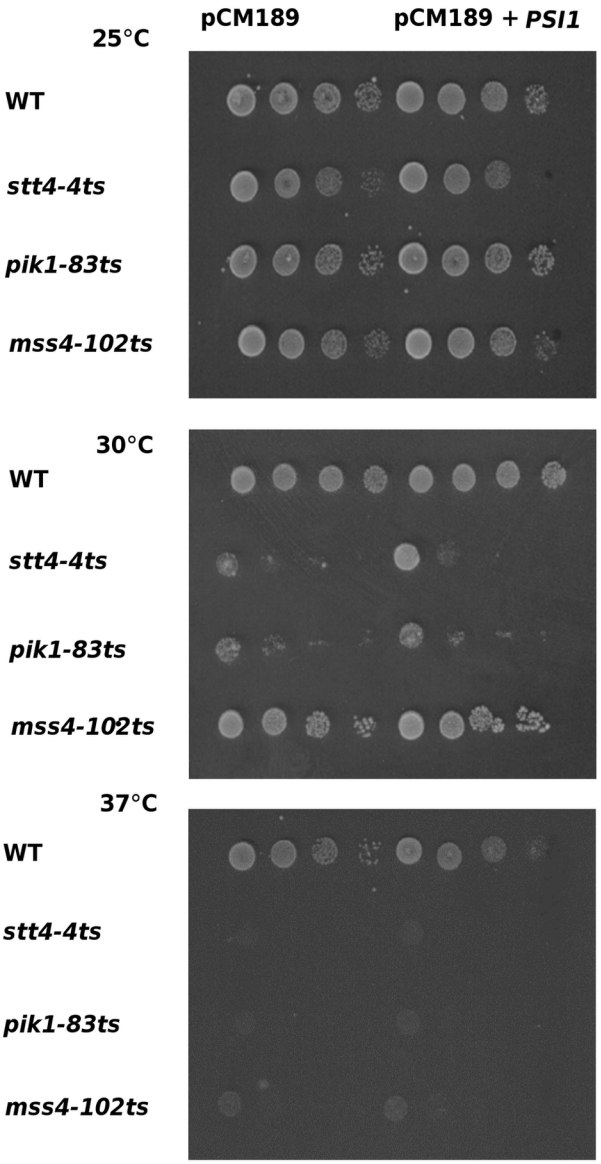

TRA_12829_Fig 3.tif

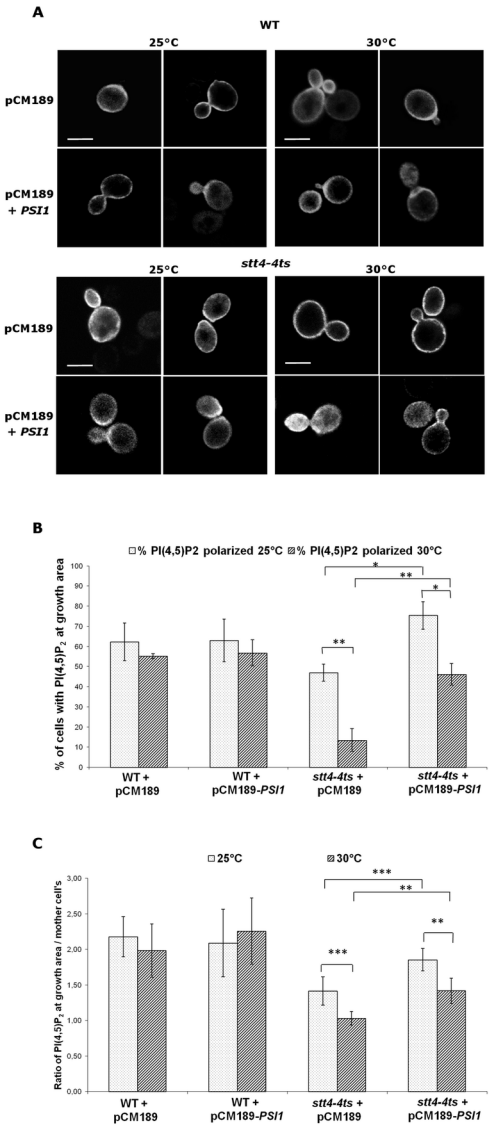

TRA_12829_Fig 4.tif

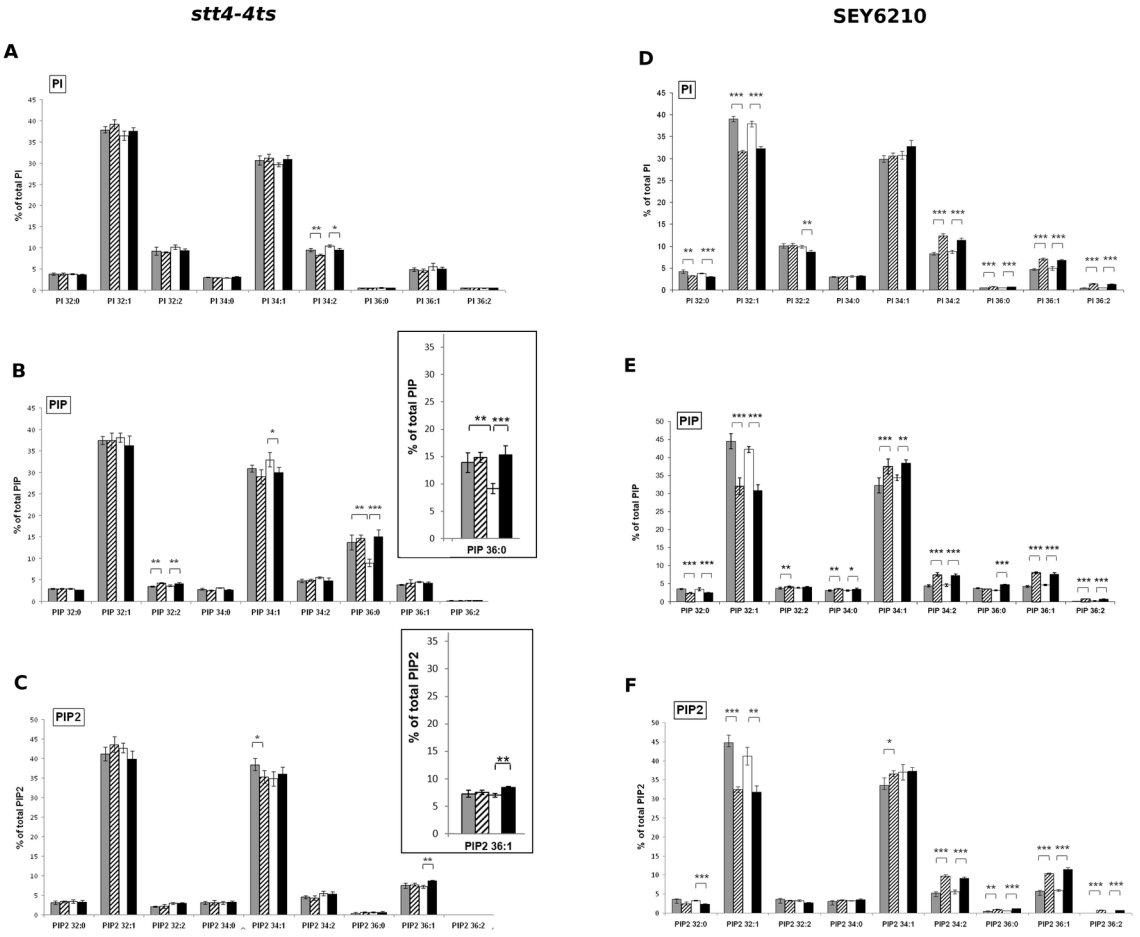

TRA_12829_Fig 5.tif

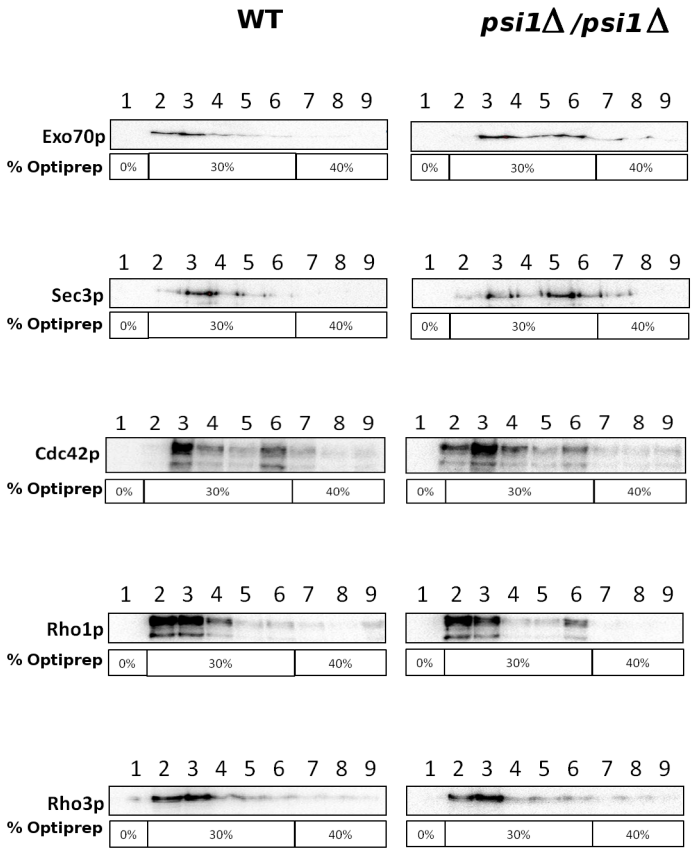

TRA_12829_Fig 6.tif

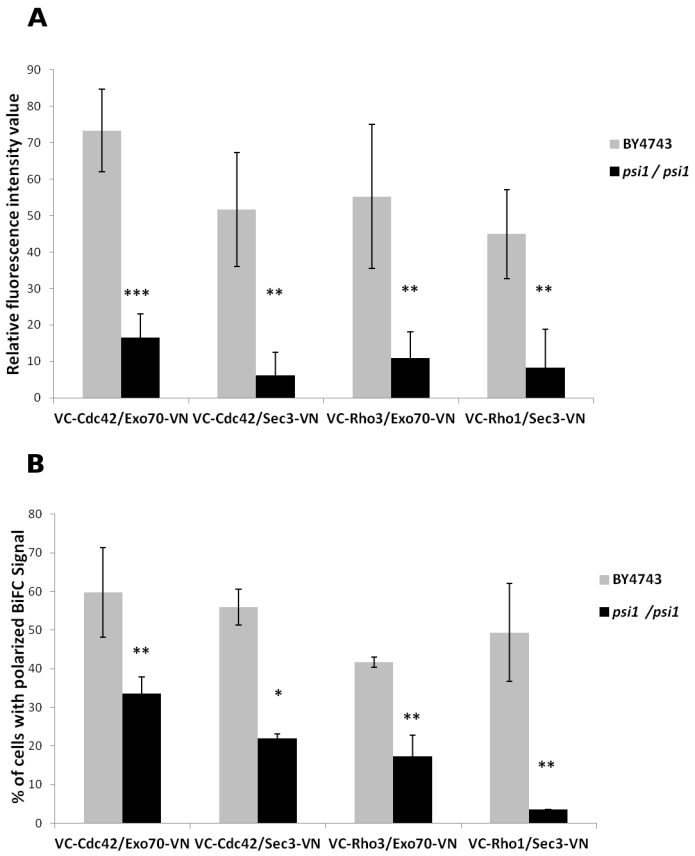

TRA_12829_Fig 7.tif

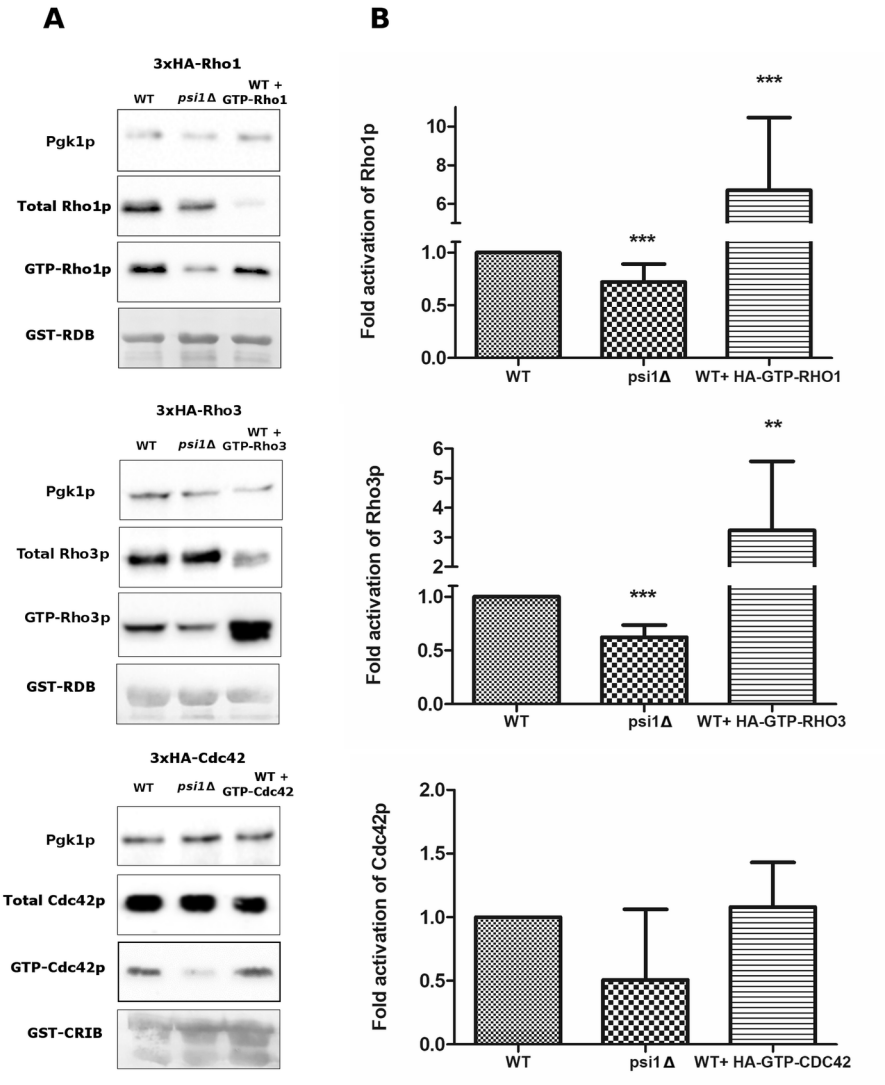

TRA_12829_Fig 8.tif

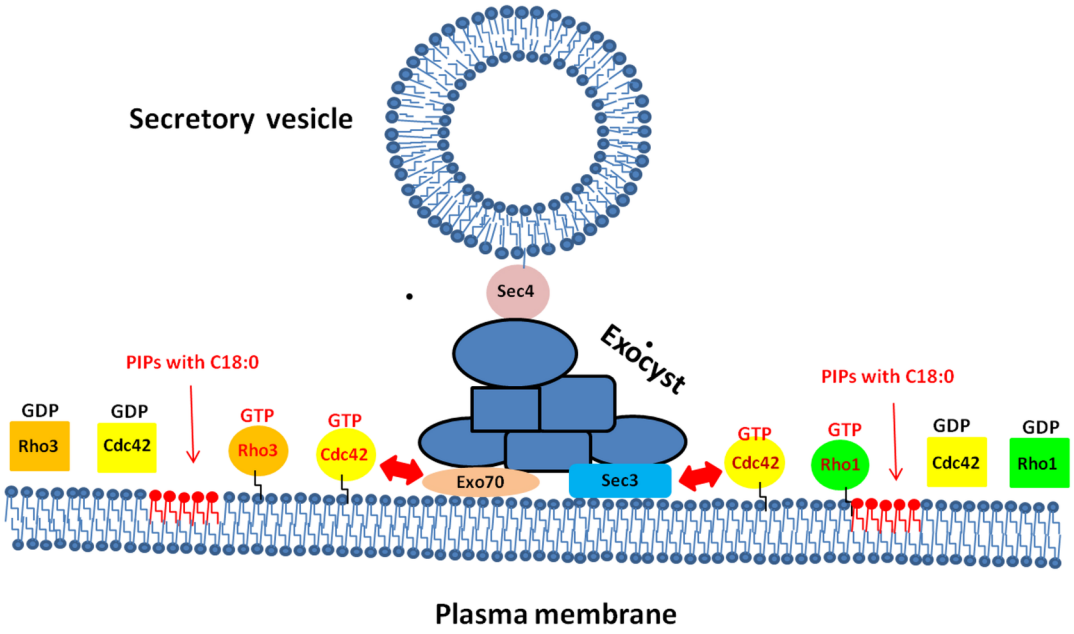

TRA_12829_Graphical abstract.tif